Pulmonary exposure to carbon nanotubes promotes murine arterial thrombogenesis via platelet P-selectin

Abderrahim NEMMAR[1], Benoit NEMERY[1], Petra VANDERVOORT[2], David DINSDALE[3], Peter H.M. HOET[1], Marc F. HOYLAERTS[2]

[1]Laboratory of Pneumology (Lung Toxicology), K.U.Leuven, Leuven, Belgium, [2]Center for Molecular and Vascular Biology, K.U.Leuven, Leuven, Belgium and [3]Medical Research Council Toxicology Unit, Leicester, United Kingdom.

Correspondence to: Prof. B. Nemery
K.U.Leuven
Laboratory of Pneumology
Unit of Lung Toxicology
Herestraat, 49
B-3000 Leuven
Belgium
e.mail: ben.nemery@med.kuleuven.ac.be

Abstract

Carbon nanotubes, having a diameter as small as a few nanometers, yet with robust mechanical properties, can be functionalized with chemical and biological agents and be used for the delivery of target DNA molecules or peptides into specific tissues. However, their potential adverse health effects remain unknown. Here, we studied the acute (24 h) effects of intratracheally administered (200 and 400 μg) multi-wall ground carbon nanotubes (CNT) on lung inflammation assessed by bronchoalveolar lavage (BAL), and peripheral arterial thrombogenicity in mice. The latter was evaluated from the extent of photochemically induced thrombosis in the carotid artery, measured via transillumination. I.t. instillation of CNT induced a dose-dependent influx of neutrophils in BAL, paralleled by enhanced experimental arterial thrombus formation. By flow cytometry, circulating platelet-leukocyte conjugates were found to be elevated 6 h after i.t. instillation of CNT. The pretreatment of mice with a blocking anti-P-selectin antibody prevented the formation of platelet conjugates in the circulation but did not affect neutrophil influx in the lung. Although P-selectin neutralization had no effect on the vascular injury triggered thrombus formation in saline-treated mice, it abrogated the CNT induced thrombotic amplification. We conclude that the CNT induced lung inflammation is responsible for systemic platelet activation and subsequent platelet P-selectin mediated thrombogenicity. Our findings uncover that newly engineered CNT affect not only the respiratory but also cardiovascular integrity, necessitating an evaluation of their potential risk for human health.

Introduction

Nanotechnology is a broad interdisciplinary area of research, grouping physical, chemical, biological and engineering expertises involved in manufacturing of materials at a sub-100 nanometer scale [1]. It is believed to have huge potential benefits in areas as diverse as drug development, information and communication technologies, and the production of stronger, lighter materials [2;3].

Despite extensive potential applications in material sciences and engineering, exposure of man to nanoparticles and nanomaterials throughout manufacturing, application and waste management necessitates investigations for potential biological hazards of such materials on health and environment[1].

Carbon nanotubes are cylindrical carbon molecules that exhibit unusual strength, display unique electrical properties and are efficient conductors of heat. They can be packed with DNA molecules or peptides after which they may deliver their contents to specific target sites, in various tissues, for therapeutic purposes [4;5]. While commercial interest in this material is leading to the development of mass production and handling facilities [3], little is known about the toxicity of this material.

However, it has been recently reported that carbon nanotubes exhibit cytotoxicity to human keratinocyte cells [6]. They can inhibit the growth of embryonic rat-brain neuron cells[7], HEK293 cells and human embryo kidney cells, by inducing cell apoptosis and decreasing cellular adhesion ability [8]. In addition, Lam and colleagues showed that intratracheal (i.t.) instillation of single-wall carbon nanotubes in mice induced persistent epithelioid granulomas and interstitial inflammation [9]. Warheit et al., [10] in rats, reported that i.t. instillation of single-wall carbon nanotubes caused transient inflammation and cell injury and resulted in the formation of multifocal granulomas centered around nanotubes,

similar to a foreign body reaction. Nevertheless, the relevance of these observations has been questioned because the formation of granulomas was suspected to be the consequence of the instillation as a bolus of agglomerated nanotubes [10]. More recently, it has been shown that i.t. administration of both multi-wall carbon nanotubes (CNT) or ground CNT to rats, stimulated lung cells to produce TNF-α, causing lung inflammation and fibrosis [11]. However, the consequences of pulmonary inflammation exposure to CNT for cardiovascular endpoints or systemic inflammation induction are unknown.

We have recently shown that nanoparticles diffuse rapidly, i.e. within 1 hour, from the lungs into the systemic circulation in hamsters [12] and in humans [13]. We have also demonstrated, in hamsters, that intravenously and intratracheally administered positively charged polystyrene nanoparticles enhance experimental thrombosis in hamsters [14;15]. In subsequent studies, we have shown that diesel exhaust particles (DEPs) cause lung inflammation accompanied by the development of a peripheral vascular thrombogenic tendency, caused by platelet sensitization. We have also demonstrated that histamine release by pulmonary mast cells plays a major role in triggering these processes [16-18].

In the present study, we have investigated the effect of acute exposure (24 h) to CNT on lung inflammation and its consequences for peripheral thrombogenicity modification, in mice. Moreover, we have investigated in more detail the extent of systemic platelet activation and have addressed the importance of platelet surface expressed P-selectin in upregulating the peripheral arterial thrombogenicity.

Material and Methods

Nanotubes

Ground multi-wall carbon nanotubes (CNT) were a gift from Prof. D. Lison (Industrial Toxicology and Occupational Medicine Unit, Université Catholique de Louvain). They were manufactured by the laboratory of Nuclear Magnetic Resonance at the Facultés universitaires Notre-Dame de la Paix in Namur. Multi-wall carbon nanotubes (15 carbon layers on average) were synthesized by the decomposition of ethylene on an alumina support doped with a cobalt–iron catalyst mixture and purified by subsequent treatment with NaOH [19]. They were ground in an oscillatory agate ball mill (Pulverisette 0, Fritsch), with a vertical vibration of 1 mm applied for 6 h. The length of individual nanotubes was significantly reduced by grinding (0.7 ± 0.07 µm vs 5.9 ± 0.05 µm), but other characteristics of the material such as average inner diameter (5.1 ± 2.1 nm vs 5.2 ± 1.5 nm), average outer diameter (11.3 ± 3.9 nm vs 9.7 ± 2.1 nm), specific surface area (307 ± 15 m^2/g vs 378 ± 20 m^2/g), oxidized forms (13.1 ± 0.7 atomic % vs 13.7 ± 0.7 atomic %) and carbon content (98.0 ± 0.2 % vs 97.8 ± 0.2) were not affected by the grinding process [11].

CNT were suspended in sterile pyrogen-free saline (NaCl 0.9 %) containing tween 80 (0.1%). To minimize their aggregation, CNT suspensions were always sonicated (Branson 1200, VEL, Leuven, Belgium) for 15 min and vortexed immediately (< 1 min) before their dilution and prior to intratracheal administration.

Samples of the CNT suspension were also applied, immediately, to formvar/carbon-coated nickel grids (300mesh). The liquid was then removed and the grids were air-dried before examination in a Zeiss 902A electron microscope. Ground CNT

Deleted: (To be completed by David)

Deleted:

Deleted: during

Deleted:

Deleted:

Deleted: Control mice received saline containing tween 80 (0.1%).

were also suspended in absolute ethanol, sonicated for 30 min and examined as described above.

Animals and intratracheal instillation of CNT

This project was reviewed and approved by the Institutional Review Board of the University of Leuven and experiments were performed in accordance with protocols approved by the Institutional Animal Care and Research Advisory Committee.

Male and female Swiss mice weighing 45-50 g, were used. They were anesthetized with sodium pentobarbital (60 mg/kg, i.p.), placed supine with extended neck on an angled board. A Becton Dickinson 24 Gauge cannula was inserted via the mouth into the trachea. The CNT suspensions (200 or 400 µg/mouse) or vehicle-only were instilled (40 µl) via a sterile syringe and followed by an air bolus of 50 µl.

Bronchoalveolar lavage (BAL) fluid analysis

Twenty-four hours following the i.t. instillation of CNT or vehicle, mice were killed with an overdose of sodium pentobarbital. The trachea was cannulated and lungs were lavaged three times with 0.7 ml (a total volume of 2.1 ml) of sterile NaCl 0.9%. The recovered fluid aliquots were pooled. No difference in the volume of collected fluid was observed between the different groups. BAL fluid was centrifuged (1,000 g x 10 min, 4°C). Cells were counted in a Thoma hemocytometer after resuspension of the pellets and staining with 1% gentian violet. The cell differentials were microscopically performed on cytocentrifuge preparations fixed in methanol and stained with Diff Quick (Dade, Brussels, Belgium). The supernatant was stored at - 80 °C until further analysis.

Experimental arterial thrombosis model

Twenty-four hours after i.t. instillation of CNT or saline, *in vivo* thrombogenesis was assessed. Following induction of anesthesia, mice were placed in a supine position on

a heating pad at 37°C, tracheotomized, and artificially ventilated (Hugo Sachs Apparatus Minivent type 845 respirator; Hugo Sachs Elektronik-Harvard Apparatus GmbH, March-Hugstetten, Germany). A 2F venous catheter (Portex, Hythe, UK) was inserted in the right jugular vein for the administration of Rose Bengal. Thereafter, the right carotid artery was exposed from the surrounding tissue and mounted on a transilluminator. After the intravenous administration of Rose Bengal (20 mg/kg), the segment of the carotid artery was irradiated with green light (540 nm) for 90 seconds, using an optic fiber mounted on a micromanipulator located 5 mm above the artery. The thrombus was monitored under a microscope at x 40 magnification. The change over time in light transmission through the blood vessel at the site of the trauma was recorded using a microscope-attached camera. Images were recorded at intervals of 10 seconds over a period of 40 minutes. Image analysis was used to quantitate thrombus intensity. The size of the thrombus was expressed in arbitrary units (A.U.) as the total area under the curve, when plotting light intensity against time [15;20;21]. The mice were euthanized at the end of the recording.

Granulocyte-platelet heteroconjugate detection

In separate animals, after i.t. instillation with saline or saline containing CNT (400 µg), blood samples were collected from the retroorbital sinus on citrate (0.4 %) containing hirudin (20 µg/ml), G4120 (1µg/ml) and prostin (1 mg/ml). To determine the existence of heteroconjugates between granulocytes and platelets via flow cytometry, 1ml of cellFix (Becton Dickinson, Franklin Lakes, NJ, USA) was added to 200 µl of blood, followed by vortexing. After 1 h fixation at room temperature, samples were centrifuged for 5 min at 2000 rpm. One ml of PBS was added to the pellet and upon vortexing, cells were centrifuged for 5 min at 1200 rpm to eliminate fixative. Thereafter, one ml of lysis buffer (Becton Dickinson, Franklin Lakes, NJ USA) was added to the pellet, and upon vortexing,

Deleted: during

cells were centrifuged for 5 min at 1200 rpm. The lysis step was then repeated. A washing step was performed by adding 1 ml of PBS to the pellet followed by centrifugation for 5 min at 1200 rpm. The pellet was then resuspended in 50 µl of PBS and 50 µl of rat serum were added, together with 5 µl of the leukocyte commun common? antigen Ly-5 marker, (=CD45?) R-phycoerythrin-conjugated rat anti-mouse antibody 30-F11 (Pharmingen, San Diego, CA) and 5 µl of platelet $\alpha_{IIb}\beta_{III}$ marker FITC-labelled rat ant-mouse integrin CD41/61 antibody MO20 (Emfret, Würzburg, Germany). Following incubation in the dark at 4°C, for 20-40 min, 0.5 ml PBS was added and sample acquisition on a FACSCalibur (Becton & Dickinson, San José, CA) was done immediately.

Deleted:

Live gating was performed on leukocyte-sized events to exclude single platelets; granulocytes were selected on the basis of their forward and side scatter characteristics, as well as CD45 positivity. Gated CD45 positive granulocytes were then analysed for the presence of bound platelets in histogram plots of platelet integrin intensity.

In vivo P-selectin neutralization in PMN influx in the lung and in peripheral arterial thrombosis

To assess the role of platelet P-selectin in CNT-induced lung inflammation and enhancement of peripheral thrombogenicity, mice were i.v. injected, through the tail vein, with 60 µg of the anti–P-selectin blocking monoclonal antibody (RB40.34; Becton Dickinson, San Diego, CA), and 10 min later saline or saline containing CNT (400 µg) was i.t. instilled. Leukocyte-platelet conjugate detection, arterial thrombosis *in vivo* and PMN influx in BAL were assessed as outlined above.

Statistics

Data are expressed as means ± SEM. Comparisons between groups were performed by one way analysis of variance (ANOVA), followed by Newman-Keuls multiple range tests. P values <0.05 are considered significant.

Results

Carbon nanotube characterization

Individual CNTs were evident in all samples examined by electron microscopy but aggregates, up to 25µm in longest dimension, were found in those prepared from saline suspensions. These aggregates may have been drying artefacts as many CNTs were coalesced around crystals of NaCl. This interpretation is consistent with the absence of such aggregates in samples prepared in ethanol (figure 1); the improved dispersion of CNTs over the grids may well reflect the lower surface tension and greater volatility of this medium. The CNTs were contorted to various degrees, no partitions were observed across the lumen but several 'T & Y' branches were present. Most individual CNTs were less than 10µm long and approximately 10nm in diameter. A small proportion (>5%) were approximately 5nm in diameter and fragments of these CNTs, some as short as 70nm, were the smallest particles detected.

Deleted: (To be completed by David)

Deleted: ¶

Deleted: (figure 1).

CNT trigger lung inflammation

Depending on the i.t. treatment performed, the cells found in BAL were primarily macrophages and PMN as specified below. Lymphocytes were not found in control mouse BAL. No other cells were observed microscopically (figure 2). Diff-Quik stain of the cells recovered in bronchoalveolar BAL fluid revealed that CNT are mainly taken up by macrophages. However, aggregates of uningested CNT were also seen (Figure 2d).

Deleted: undigested

The intratracheal instillation of CNT resulted in a marked cellular influx in the lung at doses of 200 and 400 µg/mouse. While the number of macrophages did not increase (figure 2a), PMN numbers increased 8-fold at 200 µg/mouse ($p < 0.05$) and 12-fold at 400 µg/mouse ($p < 0.05$; figure 2b).

CNT enhance experimental arterial thrombosis

Figure 3 illustrates that the intratracheal instillation of CNT induced an increase in the cumulative mass of thrombus formed *in vivo* over a 40-minute interval in a photochemically injured carotid artery. CNT induced a dose-dependent augmentation of arterial thrombosis at a dose of 200 µg per animal (+245 %, $P<0.05$) and 400 µg per animal (+350 %, $P<0.01$).

I.t. administration of CNT leads to platelet-leukocyte conjugates in circulating blood

Figure 4a shows the Forward (FSc) versus Side (SSc) scatter distribution of murine blood cells. Figure 4b illustrates the SSc versus CD45 scatter diagram; gating is performed via the cross-section of R1 (figure 4d) and R2 (figure 4b), enabling for selection of CD45 positive granulocytes, excluding monocytes and free platelets. Figure 4c, shows CD41/61 distribution in the selected granulocyte cross-sectional gate and illustrates the occurrence of heteroconjugates of platelets and granulocytes, 6h after CNT administration.

After i.t. administration of CNT (400 µg/animal), 6 h appeared to be optimal for the detection of heteroconjugates (figure 4d). No formation of conjugates was found at 3 h (measured in relation to baseline in non-treated controls, set as 100 %: 104 ± 48 % in saline control group vs 109 ± 43 % in CNT group, n = 3-4), at 12 h (110 ± 30 % in saline control group vs 100 ± 30 % in CNT group, n = 4) or at 24 h (106 ± 23 % in saline control group vs 98 ± 33 % in CNT group, n = 3).

Figure 4d shows that 6 h after i.t. administration of CNT, there was a significant increase of systemic platelet activation, as measured by the existence of platelet-leukocyte

conjugates in systemic blood (130 % in control group vs 245 % in CNT group, $p < 0.05$, $n = 6$).

Consequences of P selectin neutralization on lung inflammation and thrombosis

Pretreatment of control mice with the neutralizing antibody anti-P selectin RB.40.34 did not significantly affect the number of macrophages in BAL (figure 5a), nor reduce the degree of CNT-induced PMN infiltration (figure 5b). Yet, heteroconjugate formation measured 6 h after i.t. administration of CNT was found to be blocked (figure 6) compatible with a role for P-selectin in the heteroconjugate formation [22] and therefore confirming that systemic platelet activation is potent enough to cause α-degranulation and P-selectin mediated platelet binding to circulatory leukocytes.

P-selectin neutralization did not affect the number of platelets in saline-treated mice (Ab-treated: 659,200 ± 55,766/μL vs 641,250 ± 74,137/μL) or in CNT-treated mice (Ab-treated 718,800 ± 66,917/μL vs 715,000 ± 158,406/μL). Whereas pre-treatment with anti-P-selectin antibody had no effect on the mild thrombotic response recorded in saline-treated mice (figure 7), the CNT amplification of thrombogenesis was abrogated, in agreement with a platelet P-selectin mediated systemic activation thrombotic sensitization by CNT.

Discussion

In the present work we provide evidence that CNT deposited in the lung can upregulate lung inflammation and peripheral arterial thrombosis, the latter resulting from platelet activation, as measured via P-selectin dependent platelet-leukocyte conjugate formation in the circulation. The arterial thrombogenicity enhancement occurs within 24 hours of CNT exposure.

Pathophysiological analysis upon *in vivo* administration of high doses of *intact* CNT has proven difficult, because of mortality in about 15 % or 55 % of exposed rats (5 mg/kg) [10] or mice (16 mg/kg) [9], respectively. This effect has been explained by mechanical blockade of the upper airways by the instillate rather than by inherent toxicity of CNT [10]. Yet, recently, Muller et al. [11] have reported that CNT induce the formation of bronchial granulomas developing around focal aggregates of CNT.

Industrial use of carbon nanotubes comprises applications such as inclusion in polymers or other matrices, for which applications, an appropriate dispersion is essential and *ground* instead of intact nanotubes are used [23-25]. Except for the length of individual nanotubes, significantly reduced by grinding, other characteristics such as average diameter, specific surface area, oxidation state or carbon content are not affected by grinding [11]. Nevertheless, it has been reported that, like intact CNT, ground CNT can also cause lung inflammation and fibrosis. Lesions found were uniformly distributed, dose–dependent and persisted up to 60 days [11].

Consequently, in the present study, we have investigated the acute (24 h) effects specifically of ground CNT on pulmonary and systemic inflammation and on the risk of arterial thrombosis in mice. Unlike those studies reporting high rate of mortality after i.t. instillation of intact carbon nanotube [9;10], we did not record any mortality throughout the entire study.

Deleted:

Deleted: similarly to

Deleted: also

Deleted: were

Our data show that CNT are taken up by macrophages and cause a dose-dependent increase of neutrophil influx in BAL fluid. Similar findings have been reported in rats, 3 days after i.t. of intact or ground CNT (2.5 and 10 mg/kg) [11]. An increase of neutrophils in BAL fluid of rats lungs was observed 24 hours after exposure to single-wall CNT (5 mg/kg) in rats [10]. We have recently made similar observations in hamsters, i.t. instilled with DEP or silica particles [16;17;26].

Intratracheal instillation of a bolus of particles, although non-physiological, leads to qualitatively similar results as via inhalation, for various biologic endpoints such as pulmonary inflammation and fibrosis [27]. The i.t. instillation technique enables the delivery of an accurate dose to the lungs of each animal, facilitating dose-effect study [27] Shortcomings include the administration as a bolus as opposed to inhalation over long time intervals. The consequence of the latter on our findings remains to be established using exposure by inhalation. In hamsters, we have previously reported that i.t. administered particles are able to increase the risk of thrombosis [16;17;26]. These conclusions were essentially based on femoral vein thrombosis studies because thrombus formation could be more easily studied in conditions of low blood flow. The present model of thrombosis in the carotid artery of mice is more suited than the hamster model for the study of extrapulmonary consequences of pulmonary inflammation, because of its blood flow pattern, which is arterial. The prothrombotic "enhancement" of peripheral arterial thrombosis resulting from limited endothelial damage constitutes therefore a realistic experimental approach for human thrombosis, causal of acute myocardial infarction.

Deleted: permits to establish

Deleted: delivery

P-selectin is found in storage α-granules of platelets and endothelial cells. It plays a critical role in the interactions between platelets, endothelial cells and leukocytes, promoting leukocyte rolling on activated endothelium. Endothelial P-selectin, initiates capture and rolling of circulating leukocytes at sites of inflammation and atherosclerosis [28-

[30], but also P-selectin, expressed on platelets, has been shown to be responsible for the initial rolling of leukocytes along the inflamed endothelium and to be involved in atherogenesis [29;31-33]. To a great extent, this interaction is mediated by binding of platelet P-selectin to P-selectin glycoprotein ligand-1 (PSGL-1) expressed on leukocytes [33;33;34].

To establish a link between pulmonary inflammation and cardiovascular endpoints such as arterial thrombosis, we first investigated the existence of platelet activation in the circulation making use of the decoy function of leukocytes, upon their encounter with activated platelets [35;36]. Platelet-leukocyte conjugates were detected in blood after i.t. administration of 400 µg CNT/mouse. We found a significant increase of conjugates 6 h after i.t. instillation of CNT but not after 12 and 24 h. However, when our mice were pretreated with an anti–P-selectin blocking monoclonal antibody [37], the CNT-mediated platelet-leuckocyte conjugate formation was completely blocked, compatible with sufficient platelet activation in the circulation to trigger α-degranulation, P-selectin expression and P-selectin mediated cell interactions [31].

In the context of allergic reactions, previous studies using *in vivo* models of inflammatory reactions in the skin [38] and the peritoneal cavity [39] have demonstrated that P-selectin plays an important role in allergic inflammation soon (3-12 hours) rather than later (20-24 hours) after allergen challenge. By contrast, Pitchford et al.[37] have recently reported a role for P-selectin at both 8 hours and 24 hours after allergen challenge. However, in the present study, PMN influx in BAL was not affected by P-selectin neutralization. Whereas Pitchford et al.[37] found that P-selectin expression on the surfaces of platelets is a major requirement for pulmonary eosinophil and lymphocyte recruitment, allowing circulating platelets to bind to and stimulate leukocytes for endothelial attachment. The cells presently identified are different. In fact, we did not find lymphocytes or eosinophils in BAL of mice exposed to CNT and the inflammatory cell identified in our model is the neutrophil.

Deleted: early

P-selectin neutralization does not affect the mild thrombus formation induced by endothelial denudation of the carotid artery, showing that platelet-P-selectin is not directly involved in the control of thrombus stability. Nevertheless, abrogation of the amplification of arterial thrombogenesis at 24 h by P-selectin neutralization, shows that activated platelet P-selectin plays an essential role in the prothrombotic effect executed by CNT but at another level. A causal relationship may exist with the measured heteroconjugates. In this respect, our data are in agreement with the findings of Yokoyama et al.[31] who demonstrated an essential role for platelet P-selectin in arterial thrombogenesis, via the formation of large stable platelet-leukocyte aggregates. Priming circulating neutrophils by adhering activated platelets will further activate leukocytes and may upregulate and release enzymes such as elastase and cathepsin G which contribute to the development of a thrombotic tendency via priming platelets for a subsequent encounter with a mildly injured vessel wall eventually[26] even when these enzymes proteolytically degrade PSGL-1[40]. Leukocyte inflammation is associated with elevated microvesicle formation, positive for tissue factor. P-selectin positive microvesicles may likewise exert an inflammatory action by activating leukocytes, both phenomena probably playing a central role in thrombus formation [41]. Finally, even when degranulated platelets rapidly lose their surface P-selectin as a consequence of proteolysis, these platelets continue to circulate and may participate in the CNT-induced enhancement of thrombosis.

In conclusion, our data provide novel evidence that, within 24 h of their deposition in the lungs, CNT cause pulmonary inflammation responsible for systemic platelet activation via P-selectin dependent platelet-leukocyte conjugation and subsequent arterial thrombogenecity enhancement. Our findings provide experimental evidence that newly engineered CNT affect not only the respiratory tract but also the cardiovascular system justifying a thorough health risk assessment for carbon nanotubes.

Deleted: i

Deleted: e

Deleted: s

Deleted: likely

Deleted: after

ACKNOWLEDGEMENTS

This work was supported by the funds of the K.U.Leuven (OT/02/45) and by the Fund for Scientific Research Flanders (G.0165.03). We thank Tim Smith for the preparation of samples for electron microscopy and Prof. Jos VERMYLEN for critically reading the manuscript.

Reference List

1. Seaton, A. and K. Donaldson. 2005. Nanoscience, nanotoxicology, and the need to think small. *Lancet* 365:923-924.

2. Colvin, V. 2003. The potential environmental impact of engineered nanomaterials. *Nat Biotechnol* 21:1166-1170.

3. Mazzola, L. 2003. Commercializing nanotechnology. *Nature Biotechnology* 21:1137-1143.

4. Guo, Z. J., P. J. Sadler, and S. C. Tsang. 1998. Immobilization and visualization of DNA and proteins on carbon nanotubes. *Advanced Materials* 10:701-703.

5. Gao, H. J., Y. Kong, D. X. Cui, and C. S. Ozkan. 2003. Spontaneous insertion of DNA oligonucleotides into carbon nanotubes. *Nano Letters* 3:471-473.

6. Shvedova, A. A., V. Castranova, E. R. Kisin, D. Schwegler-Berry, A. R. Murray, V. Z. Gandelsman, A. Maynard, and P. Baron. 2003. Exposure to carbon nanotube material: Assessment of nanotube cytotoxicity using human keratinocyte cells. *Journal of Toxicology and Environmental Health-Part A* 66:1909-1926.

7. Mattson, M. P., R. C. Haddon, and A. M. Rao. 2000. Molecular functionalization of carbon nanotubes and use as substrates for neuronal growth. *Journal of Molecular Neuroscience* 14:175-182.

8. Cui, D. X., F. R. Tian, C. S. Ozkan, M. Wang, and H. J. Gao. 2005. Effect of single wall carbon nanotubes on human HEK293 cells. *Toxicology Letters* 155:73-85.

9. Lam, C. W., J. T. James, R. McCluskey, and R. L. Hunter. 2004. Pulmonary toxicity of single-wall carbon nanotubes in mice 7 and 90 days after intratracheal instillation. *Toxicological Sciences* 77:126-134.

10. Warheit, D. B., B. R. Laurence, K. L. Reed, D. H. Roach, G. A. M. Reynolds, and T. R. Webb. 2004. Comparative pulmonary toxicity assessment of single-wall carbon nanotubes in rats. *Toxicological Sciences* 77:117-125.

11. Muller, J., H. Huaux, F. Moreau, P. Misson, J. F. Heilier, M. Delos, M. Arras, A. Fonseca, J. B. Nagy, and D. Lison. 2005. Respiratory toxicity of multi-wall carbon nanotubes. *Toxicol.Appl.Pharmacol.*In press.

12. Nemmar, A., H. Vanbilloen, M. F. Hoylaerts, P. H. Hoet, A. Verbruggen, and B. Nemery. 2001. Passage of intratracheally instilled ultrafine particles from the lung into the systemic circulation in hamster. *Am.J.Respir.Crit Care Med.* 164:1665-1668.

13. Nemmar, A., P. H. Hoet, B. Vanquickenborne, D. Dinsdale, M. Thomeer, M. F. Hoylaerts, H. Vanbilloen, L. Mortelmans, and B. Nemery. 2002. Passage of inhaled particles into the blood circulation in humans. *Circulation* 105:411-414.

14. Nemmar, A., M. Hoylaerts, P. H. Hoet, J. Vermylen, and B. Nemery. 2003. Size effect of intratracheally instilled ultrafine particles on pulmonary inflammation and vascular thrombosis. *Toxicol.Appl.Pharmacol.* 186:38-45.

15. Nemmar, A., M. F. Hoylaerts, P. H. M. Hoet, D. Dinsdale, T. Smith, H. Xu, J. Vermylen, and B. Nemery. 2002. Ultrafine particles affect experimental thrombosis in an *in vivo* hamster model. *Am.J.Respir.Crit Care Med.* 166:998-1004.

16. Nemmar, A., B. Nemery, P. H. M. Hoet, J. Vermylen, and M. F. Hoylaerts. 2003. Pulmonary inflammation and thrombogenicity caused by diesel particles in hamsters - Role of histamine. *American Journal of Respiratory and Critical Care Medicine* 168:1366-1372.

17. Nemmar, A., P. H. M. Hoet, J. Vermylen, B. Nemery, and M. F. Hoylaerts. 2004. Pharmacological stabilization of mast cells abrogates late thrombotic events induced by diesel exhaust particles in hamsters. *Circulation* 110:1670-1677.

18. Nemmar, A., P. H. Hoet, D. Dinsdale, J. Vermylen, M. F. Hoylaerts, and B. Nemery. 2003. Diesel exhaust particles in lung acutely enhance experimental peripheral thrombosis. *Circulation* 107:1202-1208.

19. Willems, I., Z. Konya, J. F. Colomer, G. Van Tendeloo, N. Nagaraju, A. Fonseca, and J. B. Nagy. 2000. Control of the outer diameter of thin carbon nanotubes synthesized by catalytic decomposition of hydrocarbons. *Chemical Physics Letters* 317:71-76.

20. Kawasaki, T., T. Kaida, J. Arnout, J. Vermylen, and M. F. Hoylaerts. 1999. A new animal model of thrombophilia confirms that high plasma factor VIII levels are thrombogenic. *Thromb.Haemost.* 81:306-311.

21. Stockmans, F., J. M. Stassen, J. Vermylen, M. F. Hoylaerts, and A. Nystrom. 1997. A technique to investigate mural thrombus formation in small arteries and veins: I. Comparative morphometric and histological analysis. *Ann.Plast.Surg.* 38:56-62.

22. Palabrica, T., R. Lobb, B. C. Furie, M. Aronovitz, C. Benjamin, Y. M. Hsu, S. A. Sajer, and B. Furie. 1992. Leukocyte Accumulation Promoting Fibrin Deposition Is Mediated Invivo by P-Selectin on Adherent Platelets. *Nature* 359:848-851.

23. Pierard, N., A. Fonseca, Z. Konya, I. Willems, G. Van Tendeloo, and J. B. Nagy. 2001. Production of short carbon nanotubes with open tips by ball milling. *Chemical Physics Letters* 335:1-8.

24. Liu, C. H., H. Huang, Y. Wu, and S. S. Fan. 2004. Thermal conductivity improvement of silicone elastomer with carbon nanotube loading. *Applied Physics Letters* 84:4248-4250.

25. Fukushima, T., A. Kosaka, Y. Ishimura, T. Yamamoto, T. Takigawa, N. Ishii, and T. Aida. 2003. Molecular ordering of organic molten salts triggered by single-walled carbon nanotubes. *Science* 300:2072-2074.

26. Nemmar, A., B. Nemery, P. H. M. Hoet, N. Van Rooijen, and M. F. Hoylaerts. 2005. Silica particles enhance peripheral thrombosis - Key role of lung macrophage-neutrophil cross-talk. *American Journal of Respiratory and Critical Care Medicine* 171:872-879.

27. Driscoll, K. E., D. L. Costa, G. Hatch, R. Henderson, G. Oberdorster, H. Salem, and R. B. Schlesinger. 2000. Intratracheal instillation as an exposure technique for the evaluation of respiratory tract toxicity: uses and limitations. *Toxicol.Sci.* 55:24-35.

28. Ramos, C. L., Y. Q. Huo, U. S. Jung, S. Ghosh, D. R. Manka, I. J. Sarembock, and K. Ley. 1999. Direct demonstration of P-selectin- and VCAM-1-dependent mononuclear cell rolling in early atherosclerotic lesions of apolipoprotein E-deficient mice. *Circ.Res.* 84:1237-1244.

29. Robinson, S. D., P. S. Frenette, H. Rayburn, M. Cummiskey, M. Ullman-Cullere, D. D. Wagner, and R. O. Hynes. 1999. Multiple, targeted deficiencies in selectins reveal

a predominant role for P-selectin in leukocyte recruitment. *Proceedings of the National Academy of Sciences of the United States of America* 96:11452-11457.

30. Manka, D., S. B. Forlow, J. M. Sanders, D. Hurwitz, D. K. Bennett, S. A. Green, K. Ley, and I. J. Sarembock. 2004. Critical role of platelet P-selectin in the response to arterial injury in apolipoprotein-E-deficient mice. *Arteriosclerosis Thrombosis and Vascular Biology* 24:1124-1129.

31. Yokoyama, S., H. Ikeda, N. Haramaki, H. Yasukawa, T. Murohara, and T. Imaizumi. 2005. Platelet P-selectin plays an important role in arterial thrombogenesis by forming large stable platelet-leukocyte aggregates. *Journal of the American College of Cardiology* 45:1280-1286.

32. Diacovo, T. G., S. J. Roth, J. M. Buccola, D. F. Bainton, and T. A. Springer. 1996. Neutrophil rolling, arrest, and transmigration across activated, surface-adherent platelets via sequential action of P-selectin and the beta(2)-integrin CD11b/CD18. *Blood* 88:146-157.

33. Theilmeier, G., T. Lenaerts, C. Remacle, D. Collen, J. Vermylen, and M. F. Hoylaerts. 1999. Circulating activated platelets assist THP-1 monocytoid/endothelial cell interaction under shear stress. *Blood* 94:2725-2734.

34. McEver, R. P. and R. D. Cummings. 1997. Role of PSGL-1 binding to selectins in leukocyte recruitment. *Journal of Clinical Investigation* 100:485-492.

35. Michelson, A. D., M. R. Barnard, H. B. Hechtman, H. MacGregor, R. J. Connolly, J. Loscalzo, and C. R. Valeri. 1996. In vivo tracking of platelets: Circulating degranulated platelets rapidly lose surface P-selectin but continue to circulate and

function. *Proceedings of the National Academy of Sciences of the United States of America* 93:11877-11882.

36. Michelson, A. D., M. R. Barnard, L. A. Krueger, C. R. Valeri, and M. I. Furman. 2001. Circulating monocyte-platelet aggregates are a more sensitive marker of in vivo platelet activation than platelet surface P-selectin - Studies in baboons, human coronary intervention, and human acute myocardial infarction. *Circulation* 104:1533-1537.

37. Pitchford, S. C., S. Momi, S. Giannini, L. Casali, D. Spina, C. P. Page, and P. Gresele. 2005. Platelet P-selectin is required for pulmonary eosinophil and lymphocyte recruitment in a murine model of allergic inflammation. *Blood* 105:2074-2081.

38. Teixeira, M. M. and P. G. Hellewell. 1998. Contribution of endothelial selectins and alpha(4) integrins to eosinophil trafficking in allergic and nonallergic inflammatory reactions in skin. *Journal of Immunology* 161:2516-2523.

39. Jia, G. Q., J. A. Gonzalo, A. Hidalgo, D. Wagner, M. Cybulsky, and J. C. Gutierrez-Ramos. 1999. Selective eosinophil transendothelial migration triggered by eotaxin via modulation of Mac-1/ICAM-1 and VLA-4/VCAM-1 interactions. *International Immunology* 11:1-10.

40. Gardiner, E. E., M. De Luca, T. McNally, A. D. Michelson, R. K. Andrews, and M. C. Berndt. 2001. Regulation of P-selectin binding to the neutrophil P-selectin counter-receptor P-selectin glycoprotein ligand-1 by neutrophil elastase and cathepsin G. *Blood* 98:1440-1447.

41. Chirinos, J. A., G. A. Heresi, H. Velasquez, A. O. Soriano, W. Jy, E. Ahn, J. J. Jimenez, L. L. Horstman, A. Peter, J. P. Zambrano, and Y. S. Ahn. 2005. Leukocyte activation, platelet activation and formation of platelet leukocyte conjugates in venous thromboembolism. *Journal of the American College of Cardiology* 45:370A.

Figure legends

Figure 1. Transmission electron microscopy. (**a**) Sample of CNT, dispersed in ethanol and dried-down onto a formvar/carbon film, showing some of the range of forms present [bar = 250nm]. Details of the outlined regions are also shown (**b** & **c**).

Deleted: (To be completed by David)

Formatted

Deleted: ¶

Figure 2. Carbon nanotube (CNT)-induced lung inflammation. Numbers of macrophages (a), PMNs (b) in bronchoalveolar lavage (BAL). Diff-Quik stain of the cells recovered in bronchoalveolar BAL fluid, 24 hours after intratracheal instillation of saline (c) or 400 µg/mouse of carbon nanotube (CNT, b). BAL cells in the control group consist mainly of macrophages (c). Black arrowheads point to CNT-laden macrophages, red arrowheads identify cell-free aggregates of CNT and arrows identify PMN (d). Data are mean ± SEM (n=5-6). Statistical analysis by one-way ANOVA followed by Newman-Keuls multiple-comparison test.

Figure 3. CNT-induced peripheral thrombogenicity in the carotid artery. Cumulative thrombus size, expressed as total light intensity over 40 minutes (in arbitrary units [A.U.]), after a mild photochemical damage to the endothelium of the left carotid artery. Data were obtained 24 hours after intratracheal instillation of saline or CNT (200 or 400 µg/animal). Data are mean ± SEM (n = 6–8 in each group). Statistical analysis by one-way ANOVA followed by Newman-Keuls multiple-comparison test.

Figure 4. Granulocyte-platelet heteroconjugate analysis. Forward (FSc) versus Side (SSc) scatter distribution during flow cytometry of murine blood cells (**a**). SSc versus CD45 scatter diagram (**b**); cells gated in R1 (**b**) were backported in R2 (**a**), the cross-section of R1 and R2 enabling for selection of CD45 positive granulocytes, excluding monocytes and free platelets; CD41/61 distribution in the selected R1/R2 cross-section illustrates occurrence of heteroconjugates between granulocytes and platelets (**c**). Platelet-leukocyte conjugates were expressed as % of heteroconjugates (range between 0.52 to 0.71 %), in non-treated animals set as 100% and were assessed 6 h after intratracheal instillation of saline or saline containing CNT (400 µg per animal) in mice (**d**). Data are mean ± SEM. Statistical analysis by the unpaired Student's *t* test.

Figure 5. Lung inflammation after CNT administration in anti-P selectin antibody treated mice. Numbers of macrophages (a) and PMN (b) in BAL, 24 h after intratracheal instillation of saline or saline containing CNT (400 μg per animal) in mice with or without pretreatment with anti-P selectin antibody, RB.40.34 (60 mg/mouse intravenously). Data are mean ± SEM (n = 4–6 in each group). $p < 0.001$, $p < 0.05$ by Newman-Keuls multiple comparison test. Data for non–RB.40.34-pretreated animals are the same as in 2.

Figure 6. Systemic platelet-leukocyte conjugate inhibition by anti-P selectin antibody treatment. Platelet-leukocyte conjugates were expressed as % of heteroconjugates (range between 0.52 to 0.71 %), in non-treated animals set as 100% and were assessed 6 h after intratracheal instillation of saline or saline containing CNT (400 μg per animal) in mice with or without pretreatment with anti-P selectin antibody, RB.40.34 (60 mg/mouse intravenously). Data are mean ± SEM (n = 4–6 in each group). $p < 0.01$ and $p < 0.05$ by Newman-Keuls multiple comparison test. Data for non–RB.40.34-pretreated animals are the same as in 4.

Figure 7. Arterial thrombogenesis by CNT is abrogated by anti-P selectin antibody treatment. Cumulative thrombus size was assessed 24 h after intratracheal instillation of saline or saline containing CNT (400 μg per animal) in mice with or without pretreatment with the anti-P selectin antibody, RB.40.34 (60 mg/mouse intravenously). Data are mean ± SEM (n = 4–8 in each group). $p < 0.001$ and $p < 0.05$ by Newman-Keuls multiple comparison test. Data for non–RB.40.34-pretreated animals are the same as in 3.

Figure 1 (To be completed by David)

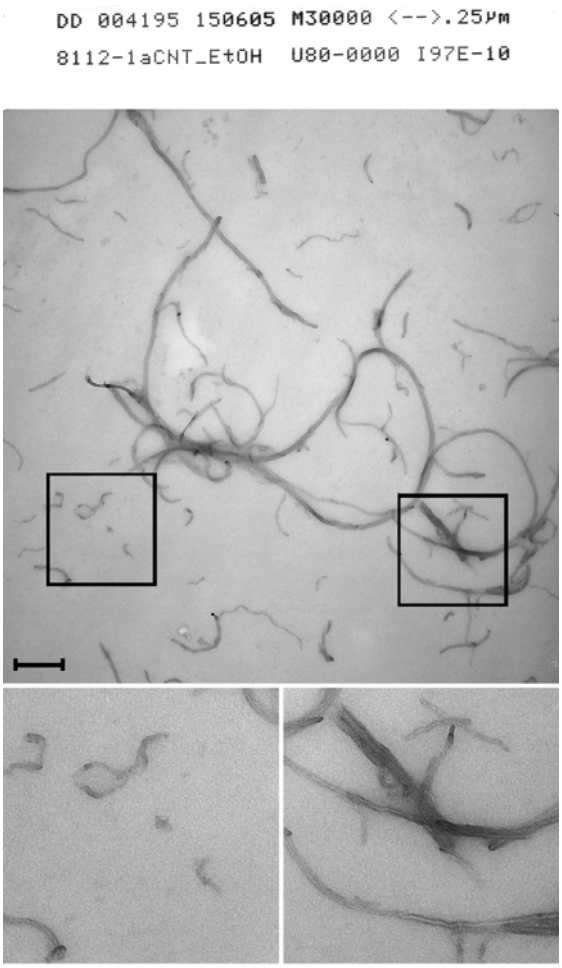

Formatted

Figure 2

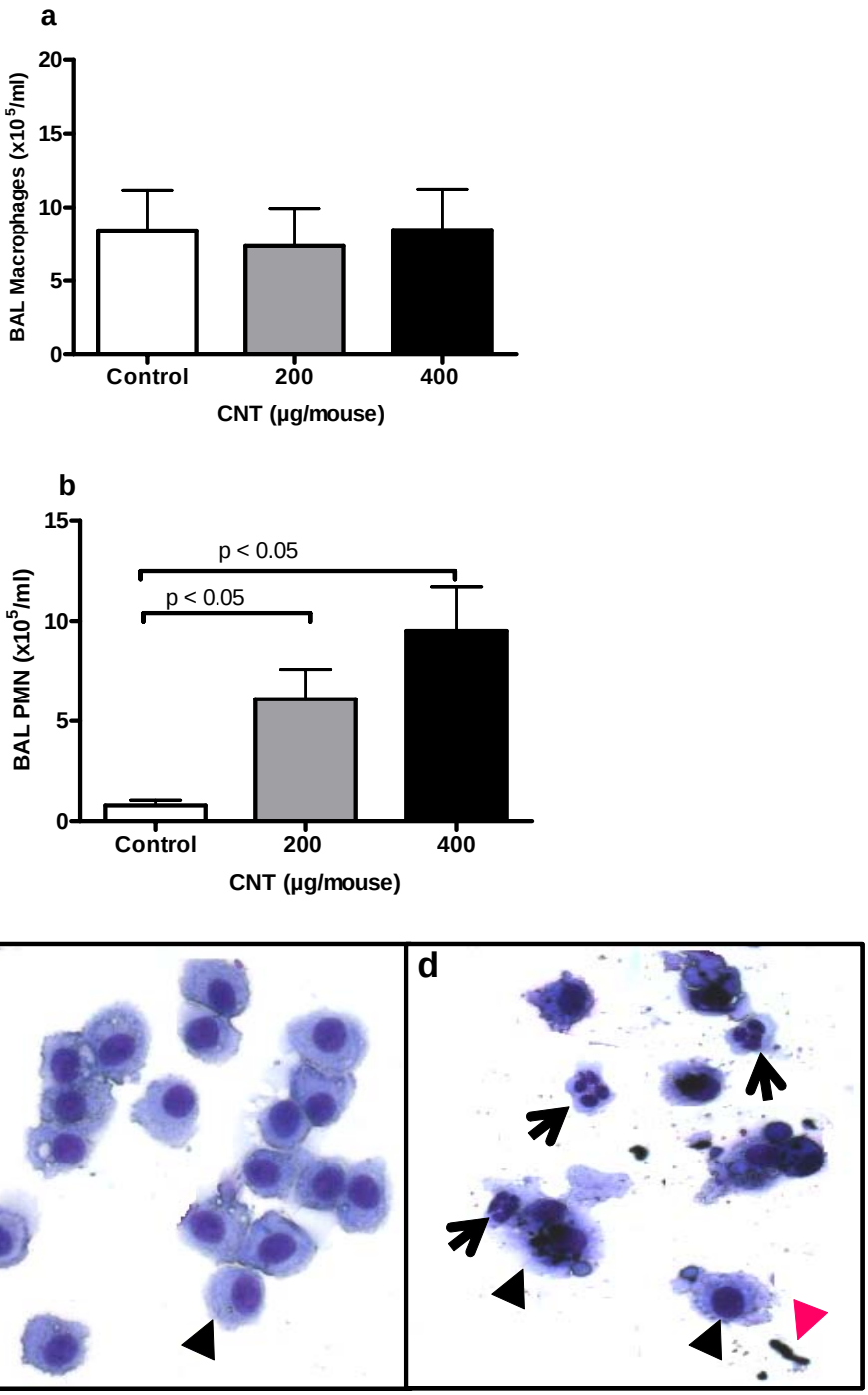
a
BAL Macrophages (x10^5/ml)
20
15
10
5
0
Control
200
400
CNT (µg/mouse)
b
BAL PMN (x10^5/ml)
15
10
5
0
p < 0.05
p < 0.05
Control
200
400
CNT (µg/mouse)
c
d

Figure 3

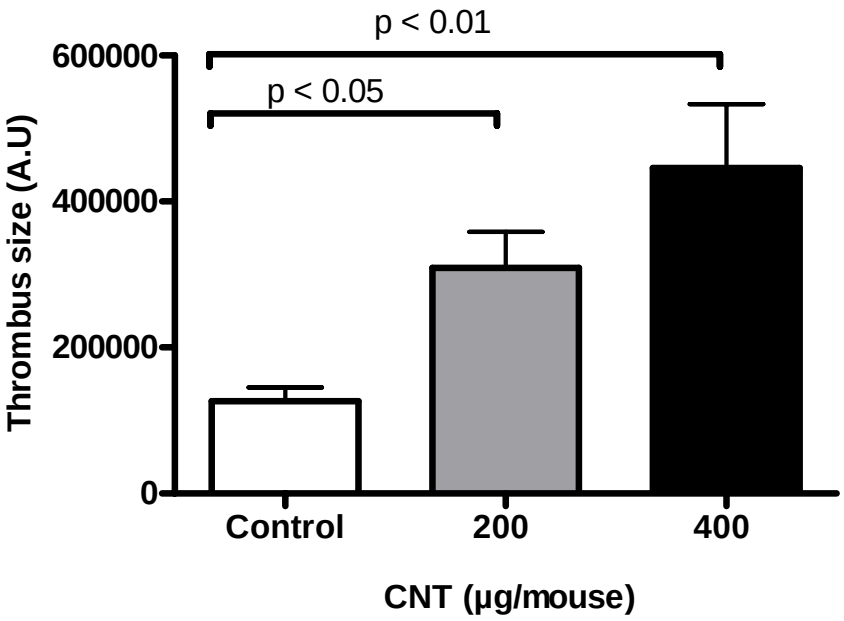
p < 0.01
p < 0.05
600000
400000
200000
0
Thrombus size (A.U)
Control
200
400
CNT (µg/mouse)

Figure 4

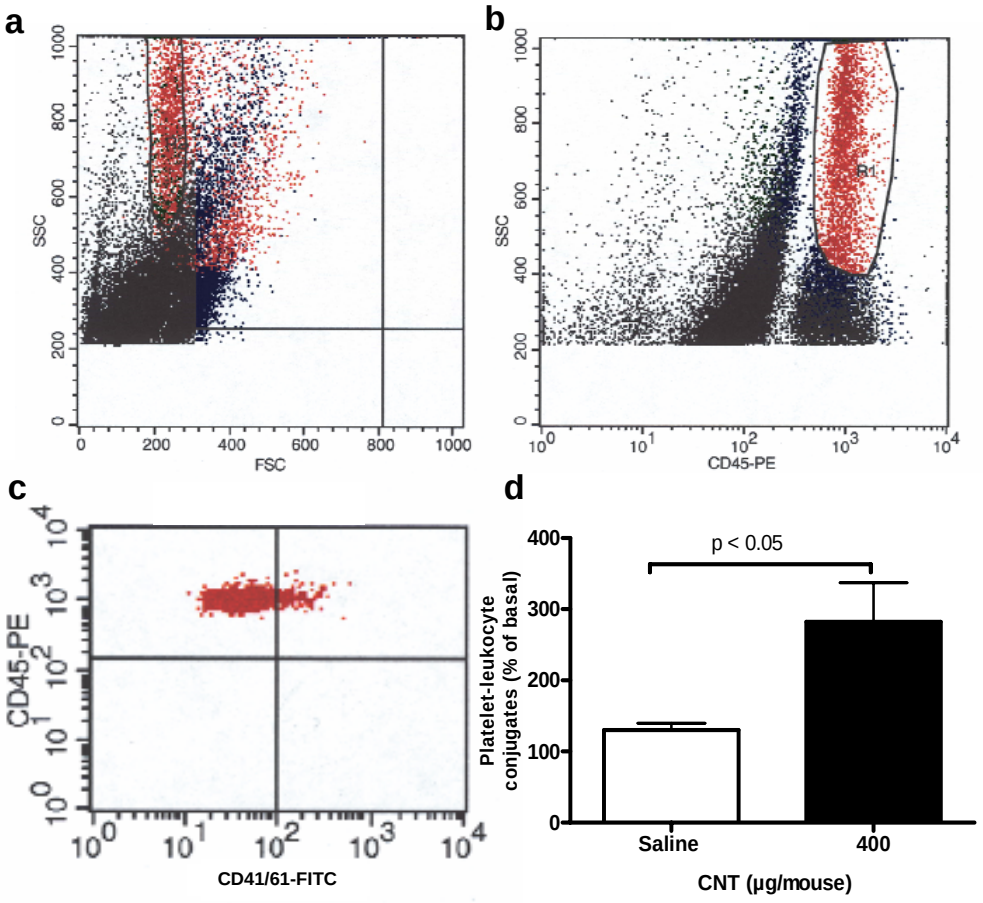
a
SSC
FSC
b
SSC
CD45-PE
R1
c
CD45-PE
CD41/61-FITC
d
Platelet-leukocyte conjugates (% of basal)
p < 0.05
Saline
400
CNT (µg/mouse)

Figure 5

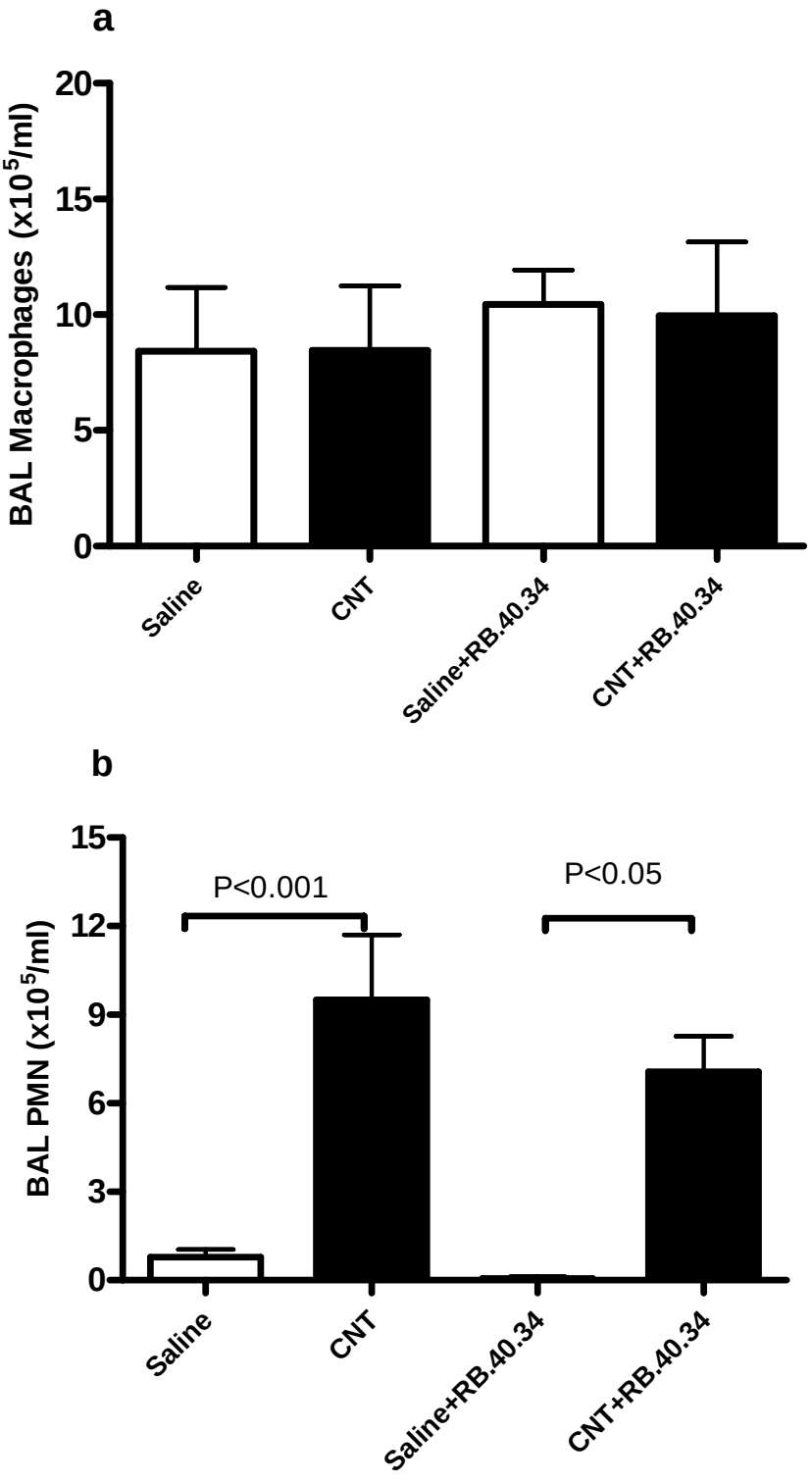
a
BAL Macrophages (x10^5/ml)
20
15
10
5
0
Saline
CNT
Saline+RB.40.34
CNT+RB.40.34
b
BAL PMN (x10^5/ml)
15
12
9
6
3
0
P<0.001
P<0.05
Saline
CNT
Saline+RB.40.34
CNT+RB.40.34

Figure 6

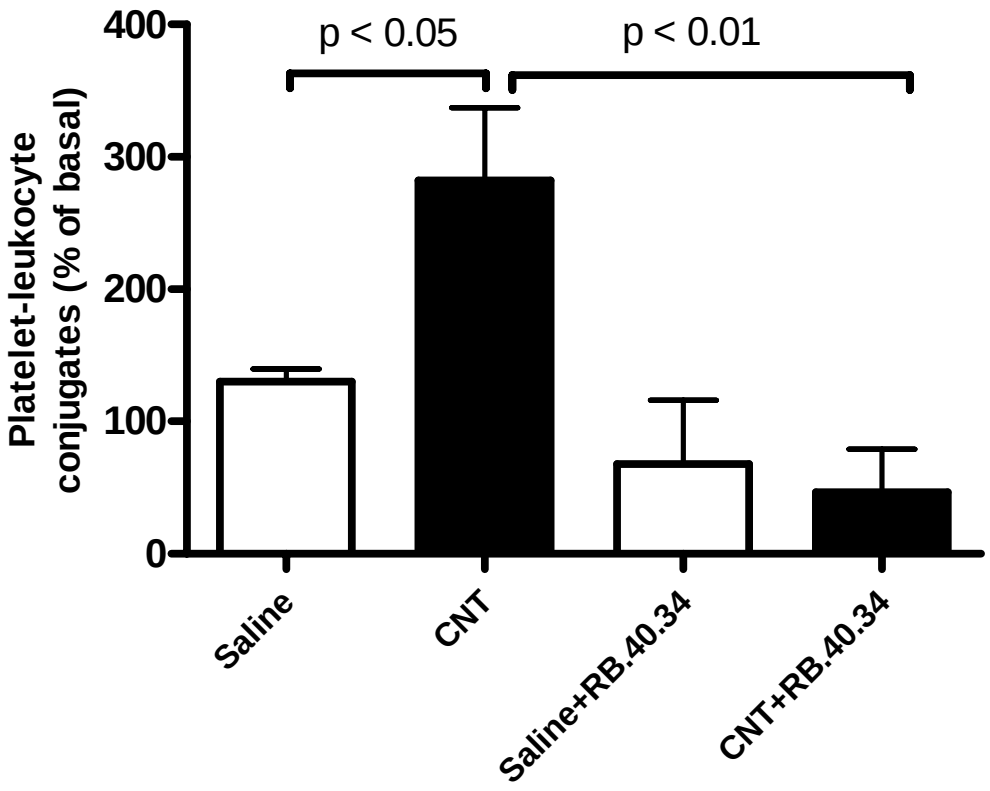
p < 0.05
p < 0.01
Platelet-leukocyte conjugates (% of basal)
400
300
200
100
0
Saline
CNT
Saline+RB.40.34
CNT+RB.40.34

Figure 7

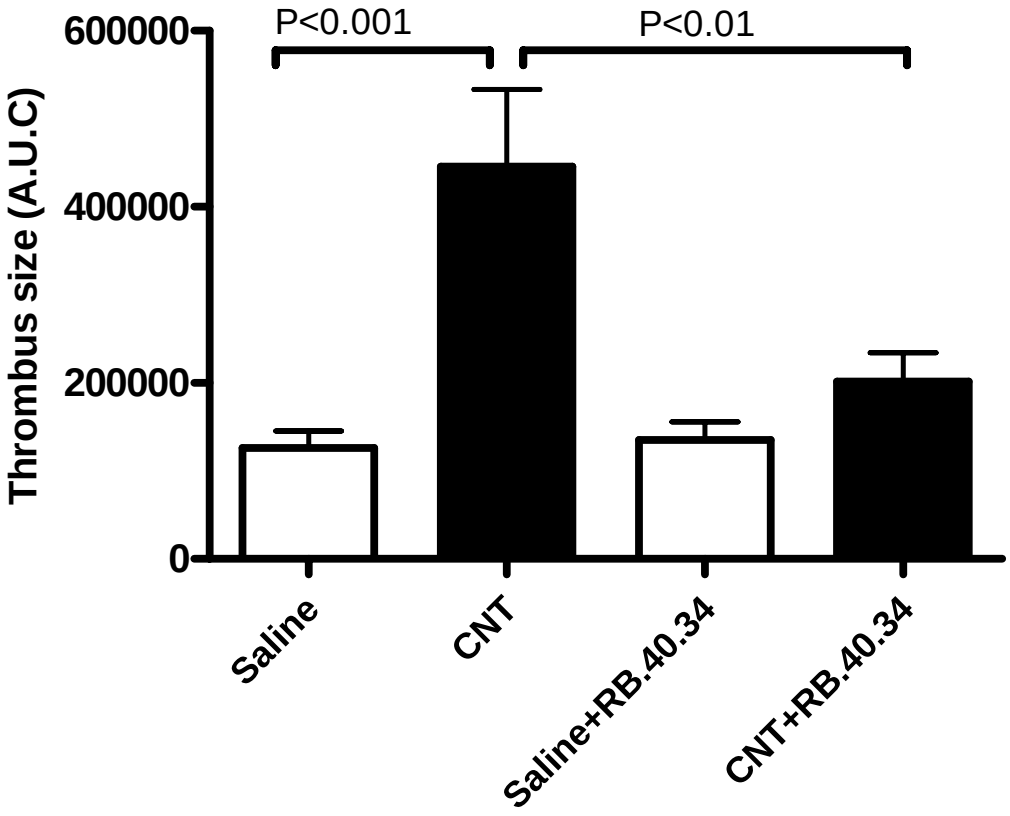
P<0.001
P<0.01
600000
400000
200000
0
Thrombus size (A.U.C)
Saline
CNT
Saline+RB.40.34
CNT+RB.40.34